

NUMERICAL SIMULATION OF FLOOD ROUTING, MODEL OF DYNAMIC EQUATIONS

LEO H. WIRYANTO¹, RATNA WIDYAWATI²

¹Department of Mathematics, Institut Teknologi Bandung,
leo@math.itb.ac.id

²Department of Civil Engineering, University of Lampung,
luh_ratnawidyawati@yahoo.co.id

Abstract. Dynamic equations of flow in a rectangular inclined channel are solved numerically for the case where the friction force of the channel wall is neglected by the gravity force. The flow discharge and the cross-section area along the channel are physical quantity that is calculated. In non-dimensional variables, the equations indicate solution in traveling wave occurring for critical flow. Near that type of flow, the perturbation method is applied to get second order equations that are first order partial differential equation with external force from the lower order equations. Numerical solution is obtained by predictor-corrector method, and the effect of these second order equations can be observed to the traveling wave, depending on the type of the flow, su-percritical or subcritical.

Key words and Phrases: Dynamic wave equation; flood routing model; perturbation method; predictor-corrector method.

1. INTRODUCTION

We consider fluid flow with flux Q entering a rectangular channel. That quantity and the cross-section area A of the channel satisfy a system of equations. Many researchers have worked in term of many models of that flow; for example in Agiralioglu [1] and Agiralioglu [2], who worked on kinematic wave for the model. Akan and Yen [3] used diffusion approximation, also in Gonwa and Kavvas [4], Ponce, Li and Simons [5], Sinha, Eswaran and Bhallamudi [6]. Another model was derived base on 1-D Saint Venant's equations, such as used and solved in Amein and Fang [7], Fread [8], Koussis [9], Lamberti and Pilati [10], Lai and Khan [11]. The equations are then called dynamic wave equation. Those authors worked for cylindrical and irregular cross-sections. For a rectangular channel with constant width, such as in Keskin and Agiralioglu [12], simplified the model becoming dynamic cascade, by neglecting some terms so that the model could be solve using an

2020 Mathematics Subject Classification: 76M10, 76M20
Received: 10-12-2021, accepted: 14-03-2022.

explicit finite different method. Barati, et. al. [13] reported the work on dynamic wave model in natural river. They analyzed the effect of the input parameter error to the output. Sulistyono and Wiryanto [14] applied the simplified model to a trapezoidal channel. For prismatic channels, Retsinis, et. al. [15] solved the model by hydrologic method. A staggered-grid finite volume method is another method that is possible to applied to the dynamic model. Sulistyono and Wiryanto [16] developed that numerical method for the dynamic model. The method is mainly used for 1-D shallow water equations, see for example in Stelling and Duinmeijer [17], Mungkasi, et. al. [18]. Instead of presenting the flood routing model in Q and A , in Sulistyono and Wiryanto [14] and also Sulistyono, et. al. [19], the authors expressed the model in similar shallow water equations, in term of the fluid depth and the velocity, but involving the variation of topography and channel width. The scheme was then used to observe the animation of the hydrograph as the effect of the geometrical channel.

Different with works in the references above, here we concern with the momentum equation of the dynamic equations. Since the channel is inclined, the gravity con-tributes in the fluid flow. But this quantity is chosen so that it makes balancing the friction force to the channel wall. This is similar for the case when the channel is without inclination and the friction is neglected, so that the momentum equation does not involve forces relating to the gravity and bottom friction. Therefore the model has constant solution. Small disturbance is then observed near that constant solution and it is indicated that the solution as the combination of two waves traveling in different direction, similar result obtained in Wiryanto and Mungkasi [20], for the case of wave generation, and the analytical solution of that problem presented in Wiryanto and Mungkasi [21].

In this work here, the character of the linear combination of waves is then used to observe the model based on the physical phenomena involving boundary condition, and it makes difficult in numerical calculation. Therefore, we use perturbation method near constant solution for the critical flow, presented by Froude number $F = 1$, based on the constant solution of the flux and the cross section. We follow in Tuck and Wiryanto [22], for the perturbation method. Characteristic method, see for example in Wiryanto [23], is then applied for the first order of the perturbation. For giving $Q(0, t)$ we obtain $Q(x, t)$ as traveling wave, and it then generates the wave of $A(x, t)$. The second order of perturbation is our main consernt as the consequence for the flow near critical one. The equations for this second order contain solution of the lower order. Discretization plays important role in designing the numerical scheme. As the result, we present the waves of Q and A . We found that the wave deformation depends on the type of the flow, supercritical or super-critical. We present some simulations in this paper.

2. PROBLEM FORMULATION

We consider fluid flow with discharge Q in an inclined rectangular channel as illustrated in Figure 1. The profile of the channel with longitudinal flow is illustrated in Figure 1a, and the cross section of the channel is illustrated in Figure 1b. The channel has constant width b and the height of the fluid is h that is the same value along the channel width, i.e. function of position x and time t , so the cross-section area is $A = hb$ and $Q = uh = ubh$. Here, $u(x, t)$ is the fluid velocity. If S_f is the friction at the channel wall and S_0 is the slop of the channel, the dynamic equations can be seen in Cunge et. al. [24] also Keskin and Agiralioğlu [12]

$$\frac{\partial A}{\partial t} + \frac{\partial Q}{\partial x} = 0 \quad (1)$$

$$\frac{\partial Q}{\partial t} + \frac{\partial Q^2/A}{\partial x} + gA \frac{\partial h}{\partial x} + gA(S_f - S_0) = 0 \quad (2)$$

Where g is the acceleration of gravity. For constant b , the third term in (2) can be written as $\frac{gA}{b} \frac{\partial A}{\partial x}$, so that the model consists of two quantities A and Q .

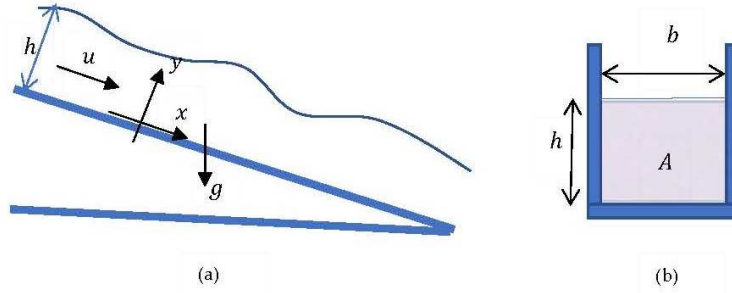


FIGURE 1. The sketch of the flow and the coordinates. (a) Longitudinal flow (b) Cross section of the channel

In case the effect of gravity, caused by inclining of the channel, can be neglected by the wall friction, i.e. $S_f \sim S_0$, the equations have any constant solution, namely A_0 and Q_0 . Based on these quantities we scale the variables. Note that the space is scaled with respect to length L and time is scaled with respect to LA_0/Q_0 . The continuity equation in nondimensional variables remains as (1) and the momentum equation becomes

$$\frac{\partial Q}{\partial t} + \frac{\partial (Q^2/A)}{\partial x} + \frac{1}{2F^2} \frac{\partial A^2}{\partial x} = 0 \quad (3)$$

Where F is Froude number, defined as $F^2 = bQ_0^2/(gA_0^3)$. Our task is to solve (1) and (3) for given initial and boundary conditions. To do so, we do some stages to analyze the solution before we develop the numerical scheme.

3. LINEARIZED MODEL

From the scaling process, now we determine the equations near the constant solution. We write

$$\begin{cases} A = 1 + A_1 \\ Q = 1 + Q_1 \end{cases} \quad (4)$$

Index indicates the order of the perturbation. We then substitute (4) into (1) and (3), then simplify the denominator to get equations

$$\begin{cases} \frac{\partial A_1}{\partial t} + \frac{\partial Q_1}{\partial x} = 0 \\ \frac{\partial Q_1}{\partial t} + 2\frac{\partial Q_1}{\partial x} + \left(\frac{1}{F^2} - 1\right) \frac{\partial A_1}{\partial x} = 0 \end{cases} \quad (5)$$

Following Wiryanto [23], (5) is written in matrix form

$$\frac{\partial \bar{w}}{\partial t} = B \frac{\partial \bar{w}}{\partial x}$$

where

$$\bar{w} = \begin{pmatrix} A_1 \\ Q_1 \end{pmatrix}, B = \begin{pmatrix} 0 & -1 \\ 1 - \frac{1}{F^2} & -2 \end{pmatrix}$$

The Eigen values and Eigen vectors of B are $\lambda_1 = -1 + \frac{1}{F}$ corresponding to $\bar{v}_1 = \begin{pmatrix} 1 \\ 1 - \frac{1}{F} \end{pmatrix}$ and $\lambda_2 = -1 - \frac{1}{F}$ corresponding to $\bar{v}_2 = \begin{pmatrix} 1 \\ 1 + \frac{1}{F} \end{pmatrix}$. We use these for diagonalizing B by introducing $\bar{w} = P\bar{y}$, where

$$P = \begin{pmatrix} 1 & 1 \\ 1 - \frac{1}{F} & 1 + \frac{1}{F} \end{pmatrix}$$

and suppose

$$\bar{y} = \begin{pmatrix} y_1 \\ y_2 \end{pmatrix}$$

so that (5) becomes uncoupled equations

$$\frac{\partial \bar{y}}{\partial t} = \begin{pmatrix} \frac{1}{F} - 1 & 0 \\ 0 & -\frac{1}{F} - 1 \end{pmatrix} \frac{\partial \bar{y}}{\partial x}$$

It has a set of solutions

$$y_1(x, t) = f_1 \left(x + \left(\frac{1}{F} - 1 \right) t \right), y_2(x, t) = f_2 \left(x - \left(\frac{1}{F} + 1 \right) t \right)$$

for any function f_1 and f_2 depending on the conditions of y_1 and y_2 . These solutions are then expressed into A_1 and Q_1 , we obtain

$$\begin{aligned} A_1(x, t) &= y_1(x, t) + y_2(x, t) \\ Q_1(x, t) &= \left(1 - \frac{1}{F}\right) y_1(x, t) + \left(1 + \frac{1}{F}\right) y_2(x, t) \end{aligned}$$

A_1 and Q_1 are linear combination between two waves that possible travel in different directions depending on F . Considering in flood routing, the boundary condition at $x = 0$ for A or Q is physically as the input, and the propagation of that condition in the flow domain is then observed. With two directions, stable numerical solution will be difficult to be obtained. We propose to observe for $F \sim 1$, and this must be followed by adding the second order of the perturbation.

4. EQUATIONS OF SECOND ORDER PERTURBATION

Instead of using expansion (4) we extend to higher order perturbation, as the effect of the perturbation of the Froude number near 1. Similar approach can be seen in [22], i.e. we write

$$\begin{cases} A = 1 + A_1 + A_2 \\ Q = 1 + Q_1 + Q_2 \\ F = 1 + F_1 \end{cases} \quad (6)$$

How much A_2 and Q_2 involved in the calculation when F_1 is given is our concern in this section. This can be obtained from the equations derived as follows. The previous process is repeated and we obtain the system of equations

$$\begin{cases} \frac{\partial A_1}{\partial t} + \frac{\partial Q_1}{\partial x} = 0 \\ \frac{\partial Q_1}{\partial t} + 2\frac{\partial Q_1}{\partial x} = 0 \end{cases} \quad (7)$$

for the first order. These equations can be solved analytically. The second equation of (7) gives

$$Q_1(x, t) = f(x - 2t)$$

for any function f . The first equation of (7) gives

$$A_1(x, t) = \frac{1}{2}Q_1(x, t)$$

Meanwhile, the second order perturbation is

$$\frac{\partial A_2}{\partial t} + \frac{\partial Q_2}{\partial x} = 0 \quad (8)$$

$$\frac{\partial Q_2}{\partial t} + \frac{\partial Q_2}{\partial x} = 2(A_1 - Q_1) \left(\frac{\partial Q_1}{\partial x} - \frac{\partial A_1}{\partial x} \right) + (2F_1 - A_1) \frac{\partial A_1}{\partial x} \quad (9)$$

The right hand side of the second equation can be expressed in Q_1 , using the analytical solution of the first order. It becomes

$$\frac{\partial Q_2}{\partial t} + \frac{\partial Q_2}{\partial x} = \left(F_1 - \frac{3}{4}Q_1 \right) \frac{\partial Q_1}{\partial x} \quad (10)$$

The function above related to Q_1 plays an important role in determining Q_2 and A_2 . Physically, we need to see the initial and boundary conditions. Since we are interested in determining the perturbation near the constant solutions, the initial condition of nondimensional variables is $A(x, 0) = 1$ and $Q(x, 0) = 1$. Therefore they give $A_1(x, 0) = 0$ and $A_2(x, 0) = 0$, so do $Q_1(x, 0) = 0$ and $Q_2(x, 0) = 0$.

As long as the initial condition is undisturbed we have constant solutions of A and Q . The disturbance can be different value of flux or cross-section area from constant solution, coming from upstream. We express this physical phenomena as the boundary condition. We give small disturbance of the flux $Q(0, t) = 1 + f(t)$ and zero disturbance to cross-section area $A(0, t) = 1$. This gives the exact solution for $Q_1(x, t) = f(x - 2t)$ and it generates wave in form of $A_1(x, t) = -\frac{1}{2}f(-\frac{1}{2}x + t)$. This is then applied to the equations (8) and (10), to see how large the effect of the Froude number to the linear solution.

5. NUMERICAL SIMULATION

In presenting the perturbation of the constant solutions $A_0 = 1$ and $Q_0 = 1$, we solve numerically (7) for the first order and then (8)-(10) for A_2 and Q_2 . First, we discretize the space $x_j = j\Delta x$ for $j = 0, 1, \dots, J$ and time $t_n = n\Delta t$ for $n = 0, 1, \dots$. Δx and Δt are small number, representing step size of the space and time. We then define $A_{1,j}^n \approx A_1(x_j, t_n)$, similarly for $Q_{1,j}^n \approx Q_1(x_j, t_n)$, $A_{2,j}^n \approx A_2(x_j, t_n)$ and $Q_{2,j}^n \approx Q_2(x_j, t_n)$.

In solving (7), characteristic method is used, see in [23]. A finite difference method of forward time forward space is applied to the second equation of (7), with $\Delta t = \frac{1}{2}\Delta x$. This is important to satisfy the characteristic line $x - 2t = \text{constant}$. This is then used to calculate the first equation of (7) formulated by finite difference equation in form of

$$A_{1,j}^{n+1} = A_{1,j}^n - \frac{\Delta t}{\Delta x} \{ (Q_{1,j+1}^{n+1} - Q_{1,j-1}^{n+1}) + (Q_{1,j+1}^n - Q_{1,j-1}^n) \} \quad (11)$$

Here, we calculate $Q_{1,j}^{n+1}$ analytically following $Q_1(x, t) = f(x - 2t)$. The result for each n above is saved and used in the finite difference equation of (10), written in

$$Q_{2,j}^{n+1} = Q_{2,j}^n - \frac{\Delta t}{\Delta x} R \quad (12)$$

where

$$R = \left\{ (Q_{2,j}^n - Q_{2,j-1}^n) - (F_1 - \frac{3}{4}Q_{1,j}^n) (Q_{1,j}^n - Q_{1,j-1}^n) \right\}.$$

This is then followed by finite difference equation of (8)

$$A_{2,j}^{n+1} = A_{2,j}^n - \frac{\Delta t}{4\Delta x} \{ (Q_{2,j+1}^{n+1} - Q_{2,j-1}^{n+1}) + (Q_{2,j+1}^n - Q_{2,j-1}^n) \} \quad (13)$$

In running the numerical scheme above, we use $\Delta x = 0.1$ and $\Delta t = 0.05$. The initial value is $A_{1,j}^0 = 0$, $Q_{1,j}^0 = 0$, and $A_{2,j}^0 = 0$, $Q_{2,j}^0 = 0$. This is followed by left boundary condition $A_{2,0}^n = 0$, $Q_{2,0}^n = 0$. As the right boundary condition, we use absorbing boundary. Therefore, the only disturbance is the left boundary condition $Q_{1,0}^n$, namely incoming hydrograph, given as

$$Q_1(0, t) = \begin{cases} \frac{1}{2} \sin(\pi t/20), & 0 \leq t \leq 10 \\ \frac{1}{2}, & 10 \leq t \end{cases} \quad (14)$$

This is not required for $A_{1,0}^n$, as it follows (11). The incoming flux will be followed by changing the elevation. We demonstrate this case to test our numerical scheme.

The informations above are used to calculate $Q_1(x, t)$, and presented in Fig. 2a. We plot Q_1 in 3-D for some values of x and t , so it can present the animation of $Q_1(x, t)$. We obtain that plot of $Q_1(x, t)$ agrees with the analytical solution described in the previous section, i.e. $Q_1(x, t) = f(x - 2t)$ where f is related to the boundary condition, in this case f is the right hand side of (14). The animation of $A_1(x, t)$ is shown in Fig. 2b, similar plot to $Q_1(x, t)$, calculated up to $t = 50$. We can see that the amplitude of A_1 is half of the amplitude of Q_1 . This confirms to the analytical solution.

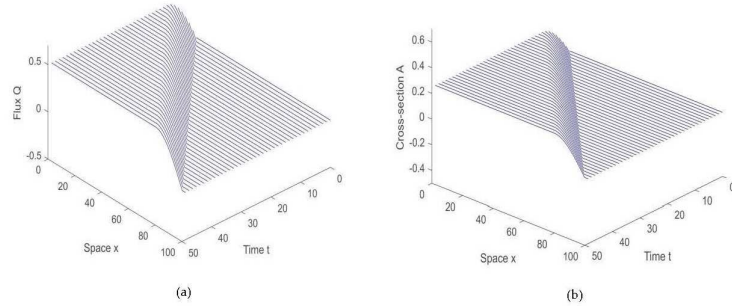


FIGURE 2. (a) Plot of some $Q_1(x, t)$ and (b) some $A_1(x, t)$ calculated using boundary condition $Q_1(0, t)$ as given in (14) with zero initial conditions for Q_1 and A_1 .

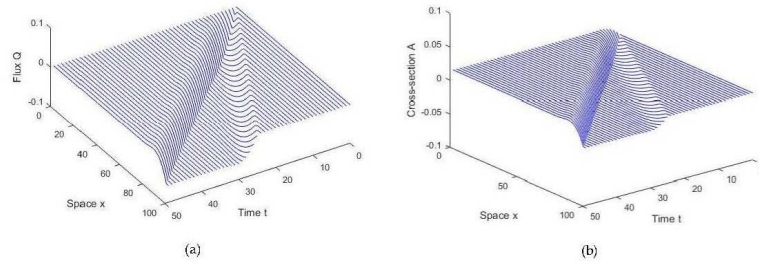


FIGURE 3. (a) Plot of some $Q_2(x, t)$ and (b) some $A_2(x, t)$ calculated using boundary condition $Q_1(0, t)$ as given in (14) with zero initial conditions for Q_2 and A_2 .

Now, the left boundary condition of Q_1 in (14) is used for calculating $Q_2(x, t)$ and $A_2(x, t)$, satisfying (8) and (10). In Fig. 3, we show plot of $Q_2(x, t)$ and $A_2(x, t)$. The Froude number F_1 and $Q_1(x, t)$ effect to the solution of (10) by appearing negative value of Q_2 at a certain interval of x , and it increases by increasing time t . It is shown in Fig. 3 for $Q_2(x, t)$ and also $A_2(x, t)$. We perform that plot as the result of our calculation using $F_1 = 0.3$. When we combine $Q_1 + Q_2$, and $A_1 + A_2$, we plot at $x = 20, 50$ and 70 as shown in Fig. 4. We can see decreasing the value of the flux and cross-section at a certain interval of time. This can be seen the curve that is less than zero. We found that $Q_1(20, t) + Q_2(20, t) < 0$ in interval $t \in [4.55, 10.55]$, then in $t \in [11.55, 25.55]$ for $Q_1(50, t) + Q_2(50, t)$ and in $t \in [16.55, 35.55]$ for $Q_1(70, t) + Q_2(70, t)$. That interval increases by increasing the position of x .

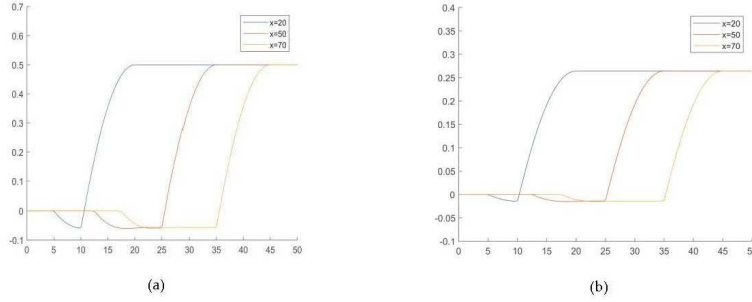


FIGURE 4. (a) Plot of $Q_1(x, t) + Q_2(x, t)$ versus t at different position x as indicated. (b) Similarly, plot of $A_1(x, t) + A_2(x, t)$ versus t . Both calculated using $F_1 = 0.3$.

The solution of Q_2 and A_2 is less contribute then A_1 , but it should be taken into account as it comes to involvement approximately up to 10%, and larger F_1 increases the percentage. For different value of F_1 , we demonstrate the model using $F_1 = -0.2$. This gives the opposite result compared to $F < 0$. We show in Fig. 5 the calculation resulting plot of $Q_1 + Q_2$ and $A_1 + A_2$ at the same positions as in Fig. 4.

The above procedure is then repeated to calculate $Q_1(x, t)$ and $A_1(x, t)$ for different left boundary condition, and we obtain similar result. Instead of (14), we use

$$Q_1(0, t) = \begin{cases} 0.1t, & 0 \leq t \leq 5 \\ 0.02(t - 10)^2, & 5 < t \leq 10 \\ 0.5, & t > 10 \end{cases} \quad (15)$$

The Q_1 -wave travels without changing the form. Meanwhile the A_1 -wave is generated by that flux following (7). The quantity of A_1 is half of Q_1 . This is then used for calculating Q_2 . The result of $Q_1(x, t) + Q_2(x, t)$ is plotted showing in Figure 5 at positions $x = 0, 20$, and 50 , for the case of $F_1 = 0.3$ shown in Fig. 6a and for $F_1 = -0.1$ shown in Fig. 6b. We can see the changing of the hydrograph at different positions and using the Froude number. We can observe the evolution of the incoming hydrograph (15), splitting into two waves and propagating in different speed. For supercritical flow of the constant solution ($F_1 > 0$), we found that the incoming hydrograph splits into two waves, where the smaller one is in front of the main wave with negative amplitude, followed by larger amplitude of the main wave rather than the incoming hydrograph. Meanwhile for subcritical flow ($F_1 < 0$), we found similar but positive amplitude for small wave, and the main hydrograph is smaller than the incoming one, i.e. measured at $x = 0$.

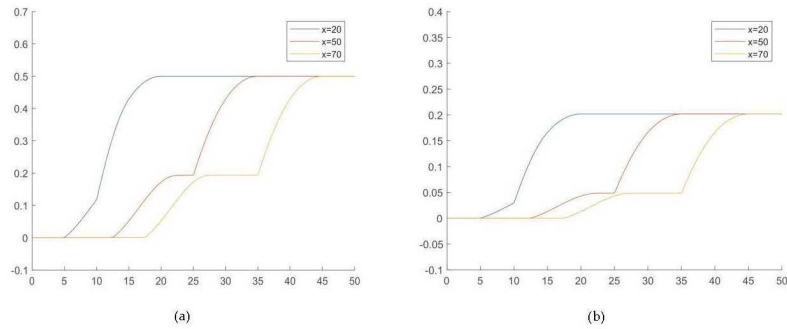


FIGURE 5. (a) Plot of $Q_1(x, t) + Q_2(x, t)$ versus t at different position x as indicated. (b) Similarly, plot of $A_1(x, t) + A_2(x, t)$ versus t . Both calculated using $F_1 = -0.2$.

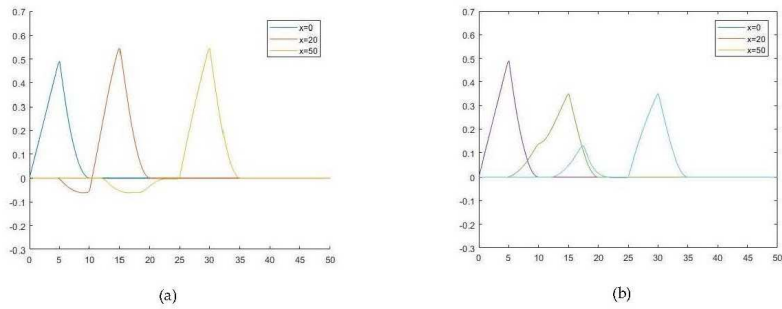


FIGURE 6. Plot of $Q_1(x, t) + Q_2(x, t)$ (vertical) versus t (horizontal) at different position x as indicated, calculated using: (a) $F_1 = 0.3$ and (b) $F_1 = -0.1$

6. CONCLUSION

Dynamic equations of flood routing have been solved numerically without involving the friction and gravity forces. The equations were firstly formulated by perturbation method. We found that the lower order of the model corresponds to the critical flow of the constant solution of the flux and the cross section. The flux propagates as travelling wave, and so does the cross section, having amplitude half of the flux. When it involves the higher order, we found that the incoming flux splits into two waves. The character depends on the flow, supercritical or subcritical. We have performed the simulation of the wave propagation.

REFERENCES

- [1] Agiralioğlu, N., "Water routing on diverging-converging watershed", *J. Hydraul.*, **107** (1981), 1003-1017.
- [2] Agiralioğlu, N., "Estimation of the time of concentration for diverging surface", *J. Hydrol. Sci.*, **33(2)** (1988), 173-179.
- [3] Akan, A.O., Yen, C.Y., "Diffusion-wave flood routing in channel networks", *J. Hydraul.*, **107** (1981), 719-732.
- [4] Gonwa, W.S., Kavvas, M.L., "A modified diffusion equation for flood propagation in trapezoidal channels", *J. Hydrol.*, **83** (1986), 119-136.
- [5] Ponce, V.M., Li, R.M., Simons, D.B., "Applicability of kinematic and diffusion models", *J. Hydraul.*, **104** (1978), 353-360.
- [6] Sinha, J., Eswaran, J.S., Bhallamudi, S.M., "Comparison of spectral and finite difference methods for flood routing", *J. Hydraul.*, textbf121(2) (1978), 108-117.
- [7] Amein, M., Fang, C.S., "Implicit flood routing in natural channels", *J. Hydraul.*, **96** (1970), 918-926.
- [8] Fread, D.L., "Technique for implicit dynamic routing in rivers with tributaries", *Water Resource. Res.*, **9(4)** (1973), 918-926.
- [9] Koussis, A., "An approximative dynamic flood routing methods", *Int. Symp. on Unsteady Flow in Open Channel*, **April 12-15th** (1976).
- [10] Lamberti, P., Pilati, S., "Flood propagation models for real-time forecasting", *J. Hydrol.*, **175** (1996), 239-265.
- [11] Lai, W., Khan, A.A., "Numerical solution of the Saint-Venant equations by an efficient hybrid finite-volume/finite difference method", *J. Hydro-dynamics*, **30(2)** (2018), 189-202.
- [12] Keskin, M.E., Agiralioğlu, N., "A simplified dynamic model for flood routing in rectangular channels", *J. Hydrol.*, **202** (1997), 302-314, [https://doi.org/10.1016/S0022-1694\(97\)00072-3](https://doi.org/10.1016/S0022-1694(97)00072-3)
- [13] Barati, R., Rahimi, S., Akbari, G.H., "Analysis of dynamic wave model for flood routing in natural rivers", *Water Sci. Eng.*, **5(3)** (2012), 243-258, doi: 10.3882/j.issn.1674-2370.2012.03.001.
- [14] Sulistyono, B.A., Wiryanto, L.H., "Investigation of flood routing by a dynamic wave model in trapezoidal channels", *AIP Conf. Proc.*, **1867** (2017), 020020, doi: 10.1063/1.4994423.
- [15] Retsinis, E., Daskalaki, E., Papanicolaou, P., "Dynamic flood wave routing in prismatic channel with hydrologic methods", *J. Water Supply: Re-search and Tech. Aqua*, **JWS 2019091** (2019).
- [16] Sulistyono, B.A., Wiryanto, L.H., "A staggered method for numerical flood routing in rectangular channels", *Adv. Appl. Fluid Mech.*, **23(2)** (2019), 171-179.
- [17] Stelling, G.S., Duinmeijer, S.P.A., "A staggered conservative scheme for every Froude number in rapidly varied shallow water flows", *Int. J. Numer. methods Fluids*, **43912** (2003), 1329-1354, doi: 10.1001/fl.537.
- [18] Mungkasi, S., Magdalena, I., Pudjaprasetya, S.R., Wiryanto, L.H., Robert, S.G., "A staggered method for the shallow water equations involving channel width and topography", *Int. J. Multiscale Comp. Eng.*, **16 (3)** (2018), 231-244.
- [19] Sulistyono, B.A., Wiryanto, L.H., Mungkasi, S., "A staggered method for simulating shallow water flows along channels with irregular geometry and friction", *Int. J. Adv. Sci. Eng. Inf. Tech.*, **10 (3)** (2020), 952-958.
- [20] Wiryanto, L.H., Mungkasi, S., "Numerical solution of wave generated by flow over a bump", *Far East J. Math. Sci.*, **100(10)** (2016), 1717-1726.
- [21] Wiryanto, L.H., Mungkasi, S., "Analytical solution of Boussinesq equations as a model of wave generation", *AIP Conf. Proc.*, **1707, 050020-1** (2016b), doi: 10.1063/1.4940852.
- [22] Tuck, E.O., Wiryanto, L.H., "On steady periodic interfacial waves", *J. Eng. Math.*, **35** (1999), 71-84.
- [23] Wiryanto, L.H., "Wave propagation passing over a submerged porous breakwater", *J. Eng. Math.*, **70** (2011), 129-136, doi: 10.1007/s10665-010-9419-3.

- [24] Cunge, J.A, Holly, F.M., Verwey, A. Jr., *Practical aspects of computational river hydraulics*, Pitman, Advanced Publishing Program (1980).